Cell Reports Medicine, Volume *5*

Supplemental information

Integrated drug profiling and CRISPR screening identify BCR::ABL1-independent vulnerabilities in chronic myeloid leukemia

Shady Adnan Awad, Olli Dufva, Jay Klievink, Ella Karjalainen, Aleksandr Ianevski, Paavo Pietarinen, Daehong Kim, Swapnil Potdar, Maija Wolf, Kourosh Lotfi, Tero Aittokallio, Krister Wennerberg, Kimmo Porkka, and Satu Mustjoki

Supplemental information:

Integrated drug profiling and CRISPR screening identify BCR::ABL1 independent vulnerabilities in chronic myeloid leukemia

Shady Adnan Awad, Olli Dufva, Jay Klievink, Ella Karjalainen, Aleksandr Ianevski, Paavo Pietarinen, Daehong Kim, Swapnil Potdar, Maija Wolf, Kourosh Lotfi, Tero Aittokallio, Krister Wennerberg, Kimmo Porkka, Satu Mustjoki

Supplementary Figure 1

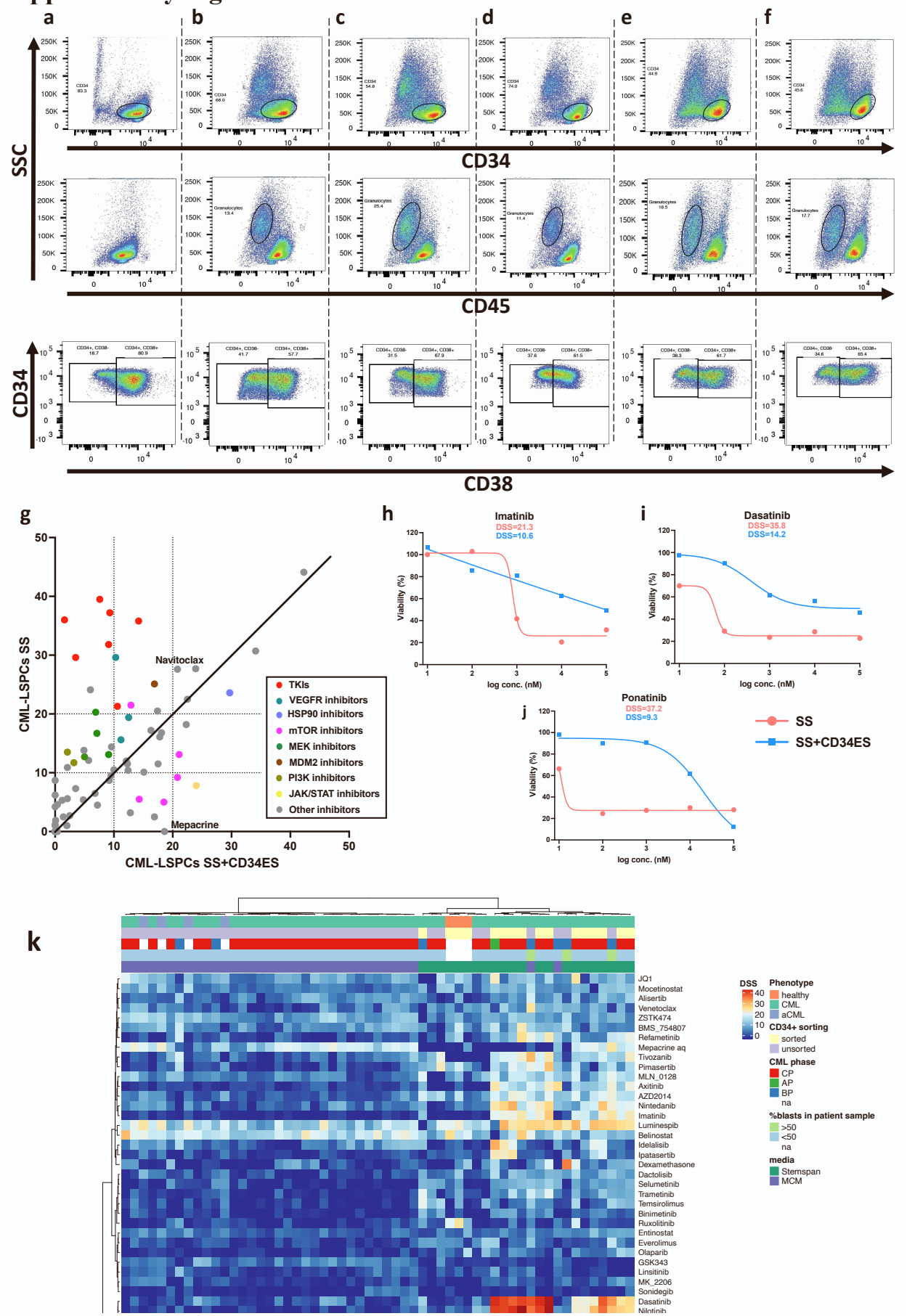

Figure S1: Effect of culturing media composition and sorting status on the drug sensitivity profile of CML-LSPCs. Related to Figure 1. Flowcytometry dot plot showing the expression of CD45, CD34 and CD38 markers on CD34+ sorted cells from a CP-CML bone marrow at a) basal, b) after 72 hours in StemSpan media, c) after 72 hours in StemSpan media supplemented by stemregenin1, d) after 72 hours in StemSpan media supplemented by stemregenin1 and UM729, e) after 72 hours in StemSpan media supplemented by commercial CD34 expansion cocktail, f) after 72 hours in StemSpan media supplemented by commercial CD34 expansion cocktail, stemregenin1 and UM729. StemSpan media with no additional supplementation was selected for subsequent experiments, because it achieved the best balance between viability maintaining and minimizing differentiation. g) Correlation of drug sensitivity scores (DSS) of LSPCs cultured in stemspan media (SS) and stemspan media supplemented with CD34+ expansion cytokine cocktail (SS+CD34ES). Dose response curve comparing LSPCs response to h) imatinib, i) dasatinib, j) ponatinib, when cultured in SS media (red) versus SS+CD34ES (Blue). Viability is normalized and expressed as percentage of viability of cells in DMSO-treated wells. Our data shows that cytokine supplements that support LSCs ex vivo expansion can also push cells to differentiate, activate several BCR-ABL independent pathways, and affect DSRT profiles even when initially use CD34+ sorted samples. Cytokine-induced differentiation was associated with the loss of sensitivity to TKIs and other functional classes such as VEGFR and AKT inhibitors, with increased activity of some mTOR and JAK inhibitors. k) Heatmap of DSS scores of 39 drugs from 57 samples, including 50 CML, 4 atypical CML (Philadelphia negative) and 3 healthy donors. Ex-vivo DSRT experiments were done using either stemspan (SS) or mononuclear cell media (MCM). A subset of CML samples was sorted for CD34+ cells. Part of this data (unsorted CML data) was previously published.(1) Explanatory tracks from above are disease status, sorting status, CML phase, blast percentage in the initial sample (prior to processing/sorting), and media used in the experiments.

Supplementary Figure 2

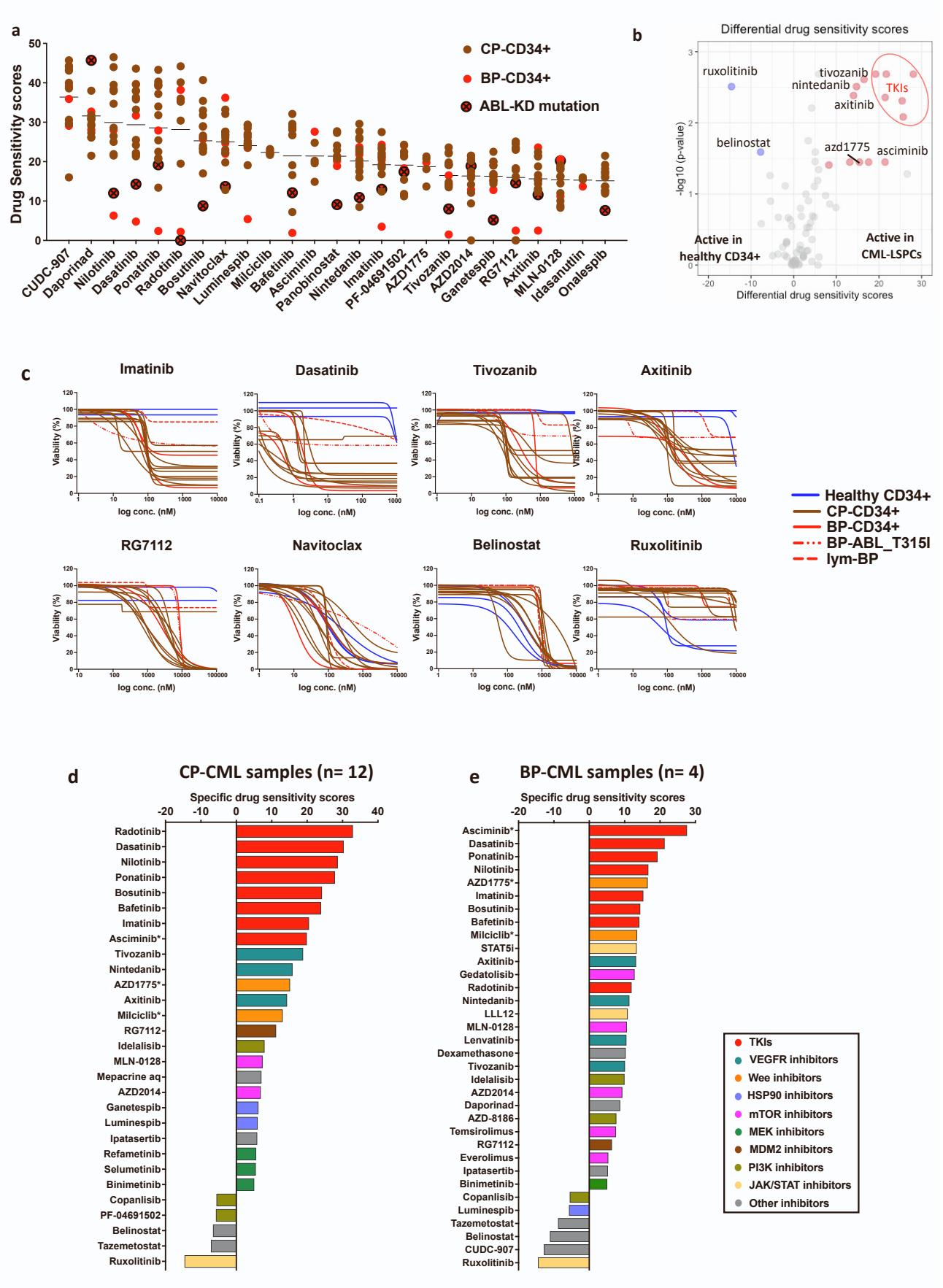

Figure S2: Drug sensitivity profiles of CML-LSPCs. Related to Figure 1. a) Dot plot showing DSS scores of the top 25 drugs in CML-LSPCs samples (n=16). Each dot represents an individual sample and is colored according to CML phase, brown for CP and red for AP/BP. Additionally, a BP-patient with ABL T315I mutation is marked with (x). Milciclib, asciminib, azd1775, idasanutlin were tested in a subset of samples. b) Volcano plot comparing DSS scores of CML-LSPCs and healthy CD34+ samples. Drugs with significantly higher activity in CML-LSPCs are highlighted in red and those active in healthy CD34+ are highlighted in blue. TKIs (imatinib, dasatinib, nilotinib, ponatinib, bosutinib, radotinib) are circled with a red circle in the figure. Comparison of DSS scores is done using non-parametric Mann-Whitney testing. FDR values (adjusted p-values for multiple comparisons) <0.15 are considered significant. c) Dose response curves showing response of individual response curves of CP (brown, n=12), BP (red, n=4), and healthy CD34+ (blue, n=3) samples to selected drugs. BP patient with T315I mutation and lymphoid BP patient curves are marked with different dashed lines. Bar plot of the differential drug sensitivity of e) CP-LSPCs (n = 12), and f) BP-LSPCs (n=4) compared to healthy CD34+ (n=3). Drugs are colored by their functional classes. (*) indicates drugs that were tested only in a subset of samples.

Supplementary Figure 3

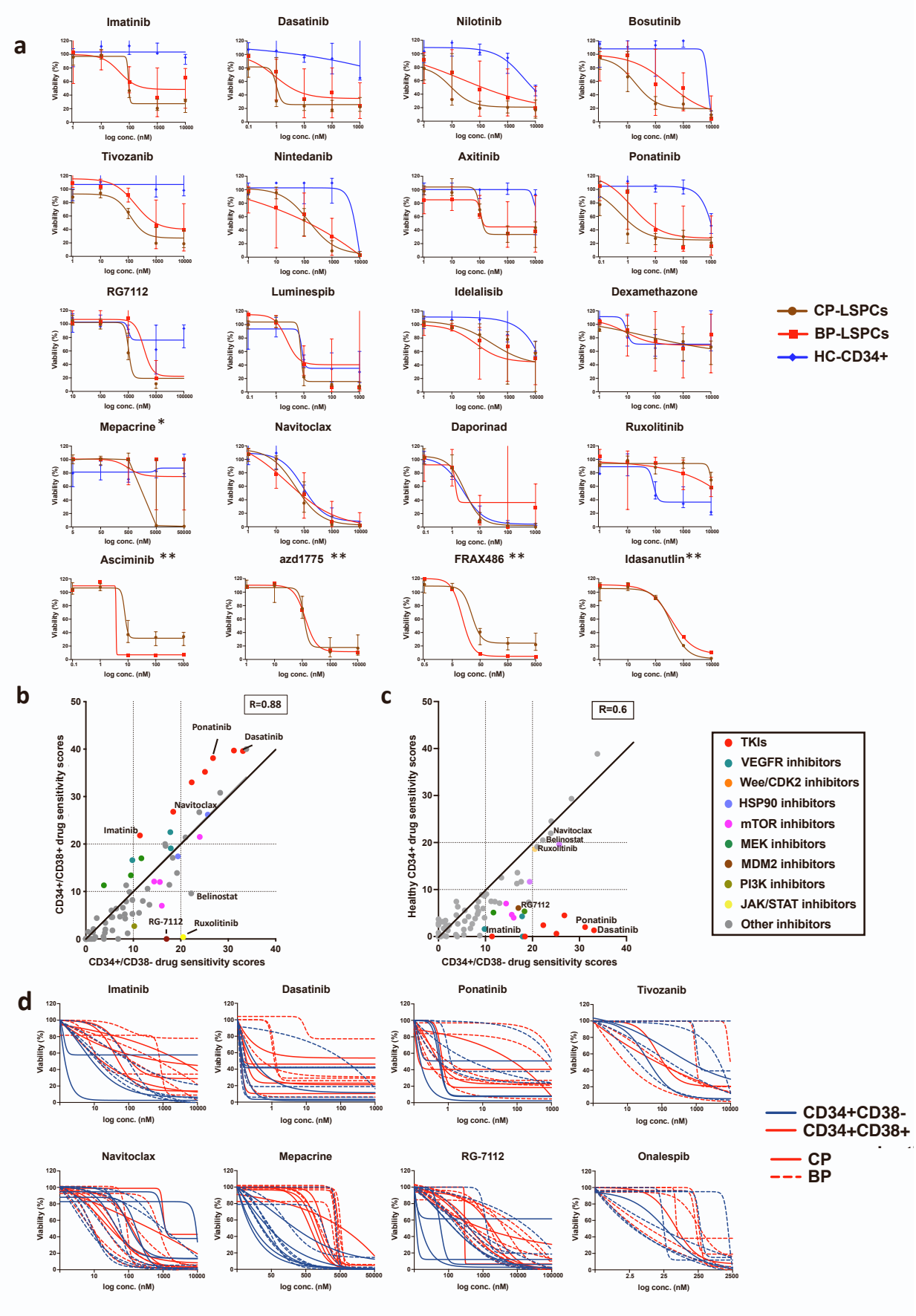

Figure S3: Differential drug activities in CML-LSPCs and healthy CD34+. Related to Figures 1 and 2. a) Dose response curves showing response of CP-LSPCs (brown), BP-LSPCs (red), and healthy CD34+ (blue) to 20 drugs. Dots represent median viability values for each drug concentration and the error bars represent the interquartile ranges. (*) For mepacrine, curve fitting model perform poorly in fitting all dose responses in CP-LSPCs. So, a line connecting dose responses was used instead. (**) indicates drugs that were tested only in a subset of samples. Dot plot showing the correlations of DSS scores between b) CML-LSCs (CD34+CD38-) and CML-LPCs (CD34+CD38+), and c) CML-LSCs and healthy CD34+ cells. Drugs are colored according to their targeting functional classes as indicated. d) Dose response curves showing individual responses of LSCs (blue), LPCs (red), of CP patients (solid curves) and BP patients (dashed curves) to the drugs shown in figure 2b.

Supplementary Figure 4

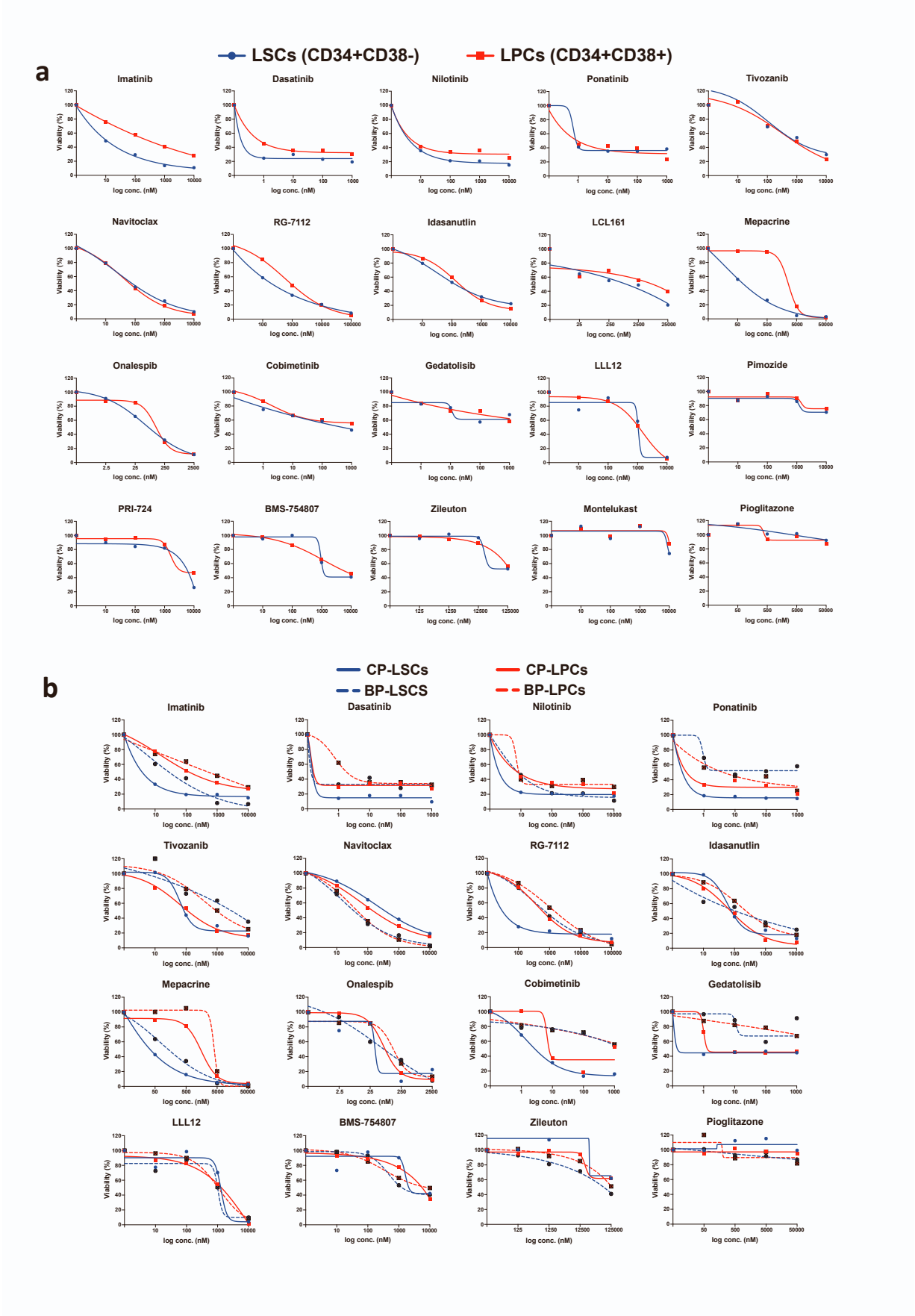

Figure S4: Flowcytometry-based drug sensitivity profiles of CML-LSCs, CML-LPCs. Related to Figure 2. a) Dose response curves showing response of LSCs (blue), LPCs (red) from 12 CML patient' samples to 20 drugs. B) Phase specific dose response curves showing response of LSCs (blue), LPCs (red), of CP patients (n=6, solid curves, and dots) and BP patients (n=6, dashed curves, x-centered dots) to 16 drugs.

Supplementary Figure 5

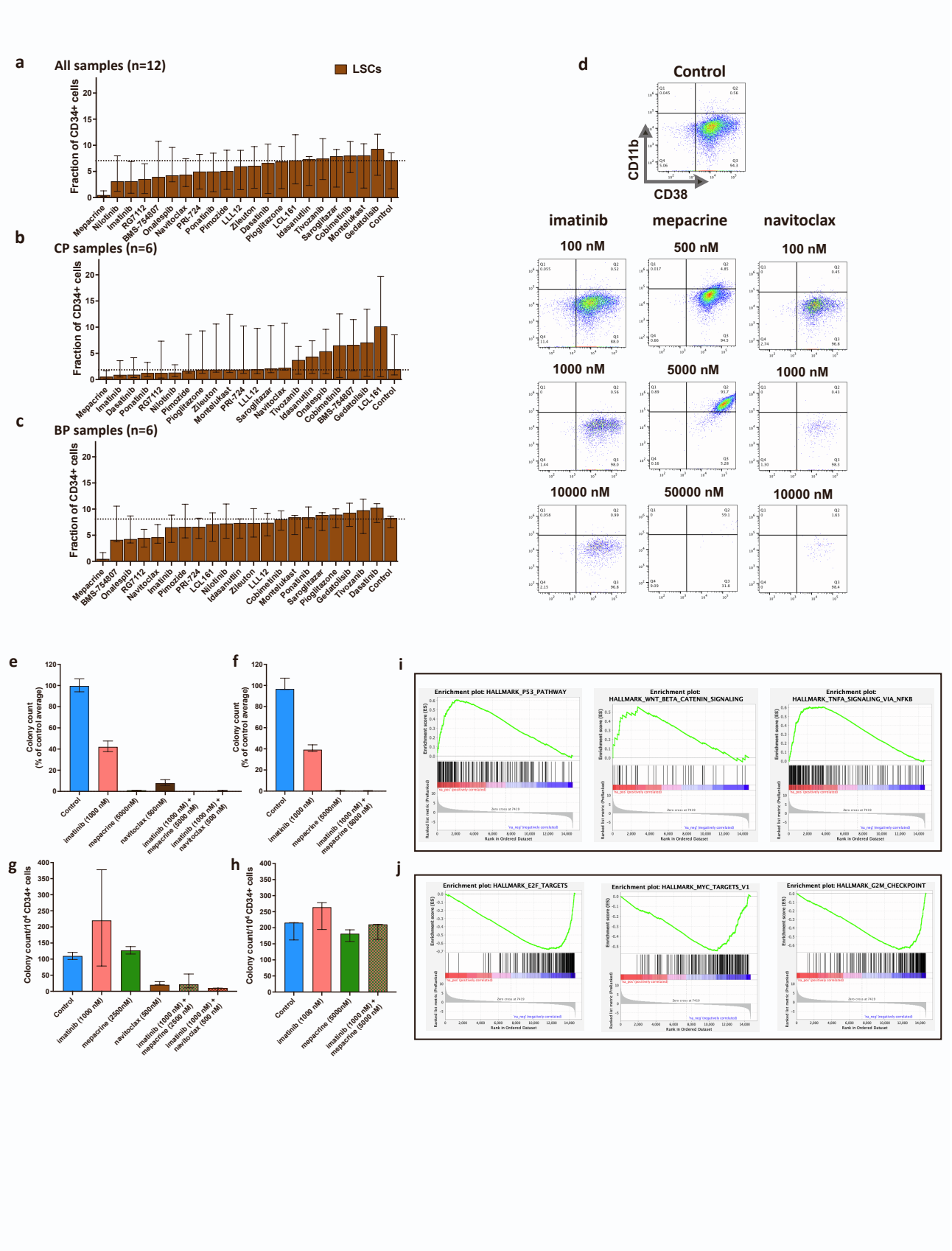

Figure S5: Flowcytometry-based drug profiling highlights mepacrine's specific targeting of primitive CML-LSCs.

Related to Figure 2. Bar plots showing the response of LSCs (CD34+CD38-) cells to the tested drugs in a) all samples, b)

CP samples, c) BP samples. The percentage of LSCs fraction of total CD34+ cells in the 3rd concentrations of all tested drugs are compared to the percentage in control (DMSO) wells. A dashed line indicates the median of control wells. Bar height represent median values with error bars representing the interquartile range. d) Flowcytometry panels showing the expression of myeloid differentiation markers CD38 (*x-axis*) and CD11b (*y-axis*) on CD34+ gated cells from imatinib, mepacrine and navitoclax treated CML cells over 3 log concentrations. e-f) Colony forming assay (CFA) (patient number=2, each is shown in a separate plot) and g-h) long term culture initiating cells (LTC-IC) assay (patient number=2, each is shown in a separate plot) of CML-LSPCs in the presence of imatinib, mepacrine and navitoclax as individual drugs and imatinib-drug combination at the indicated concentrations. Colony count output is expressed as percentage of the drug-treated conditions from control (dmso-treated) condition in CFA analysis. For LTC-IC the colony count is normalized to be expressed as colony count per 10^4 input CD34+ LSPCs. Each experiment is done in replicate (replicates are shown separately in the figure) using 2 different patient samples. A suboptimal mepacrine concentration (2500nM) was used in the 1st LTC-IC experiment (panel g) since the 5000 nM concentration used in CFA (panel e) wiped out all cells. For the 2nd LTC-IC experiment (panel h), the 5000nM mepacrine concentration was used for a shorter overnight incubation period rather than 48 hours used in the 1st experiment. i,j) Pathway enrichment figures showing the enriched pathways from gene set enrichment analysis (GSEA) from i) upregulated and j) downregulated differentially expressed genes between mepacrine and DMSO treated CML-LSPCs.

Supplementary Figure 6

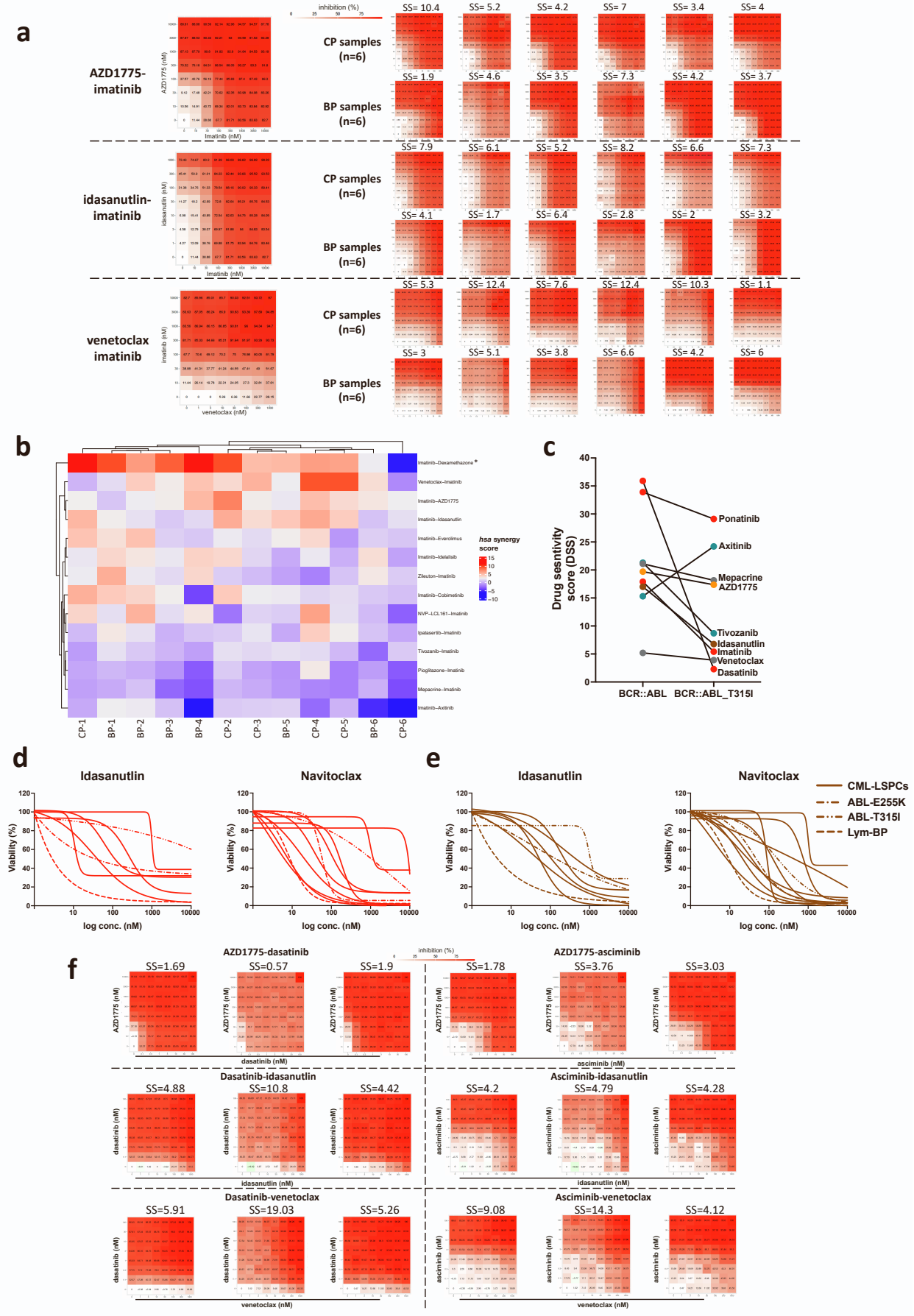

Figure S6: Drug combination screening identified AZD1775, idasanutlin and venetoclax as promising candidates for combinations with TKIs. Related to Figure 3. a) Heatmaps of dose-combination responses in CML-LSPCs samples, including 6 BP and 6 CP-LSPCs, for the most synergistic imatinib-drug combinations (AZD1775-imatinib, idasanutlin-imatinib, venetoclax-imatinib). An example heatmap is shown on the left for each imatinib-drug combination with percent inhibition values are indicated in the heatmaps. Heatmaps from the 12 individuals are shown on the right with HSA synergy score indicated on the top of each heatmap. b) Heatmap of synergy scores of 18 imatinib-drug combinations in CML-LSPCs samples (n=12). Synergy score >5 is considered synergistic, and >10 is highly synergistic. (*) imatinib-dexamethasone combination showed universally high synergistic score in all samples, which can be a technical outlier (dose-response curves seem to converge, suggesting no real synergy). c) Dot plot showing comparison of drug DSS scores from Ba/f3 cells transduced with either p210 BCR::ABL1 wild type or T315I mutant form. d-e) Dose response curves showing individual FC-DSRT responses of d) LSCs (red), e) LPCs (brown) of CML patients. Dose response curves of CML- samples are represented in solid lines, except for BP samples with ABL1-KD mutations (T315I, E255K) and lymphoid BP patient that are marked with different dotted/dashed curves as indicated. f) Heatmaps of dose-combination responses in 3 CP-LSPCs samples, for the combinations of AZD1775, idasanutlin, and venetoclax with either dasatinib or asciminib (examples of second or third line TKIs respectively). Heatmaps from individual samples are shown with percent inhibition values are indicated in the heatmaps and with HSA synergy score indicated on the top of each heatmap. Synergy score >5 is considered synergistic, and >10 is highly synergistic.

Supplementary Figure 7

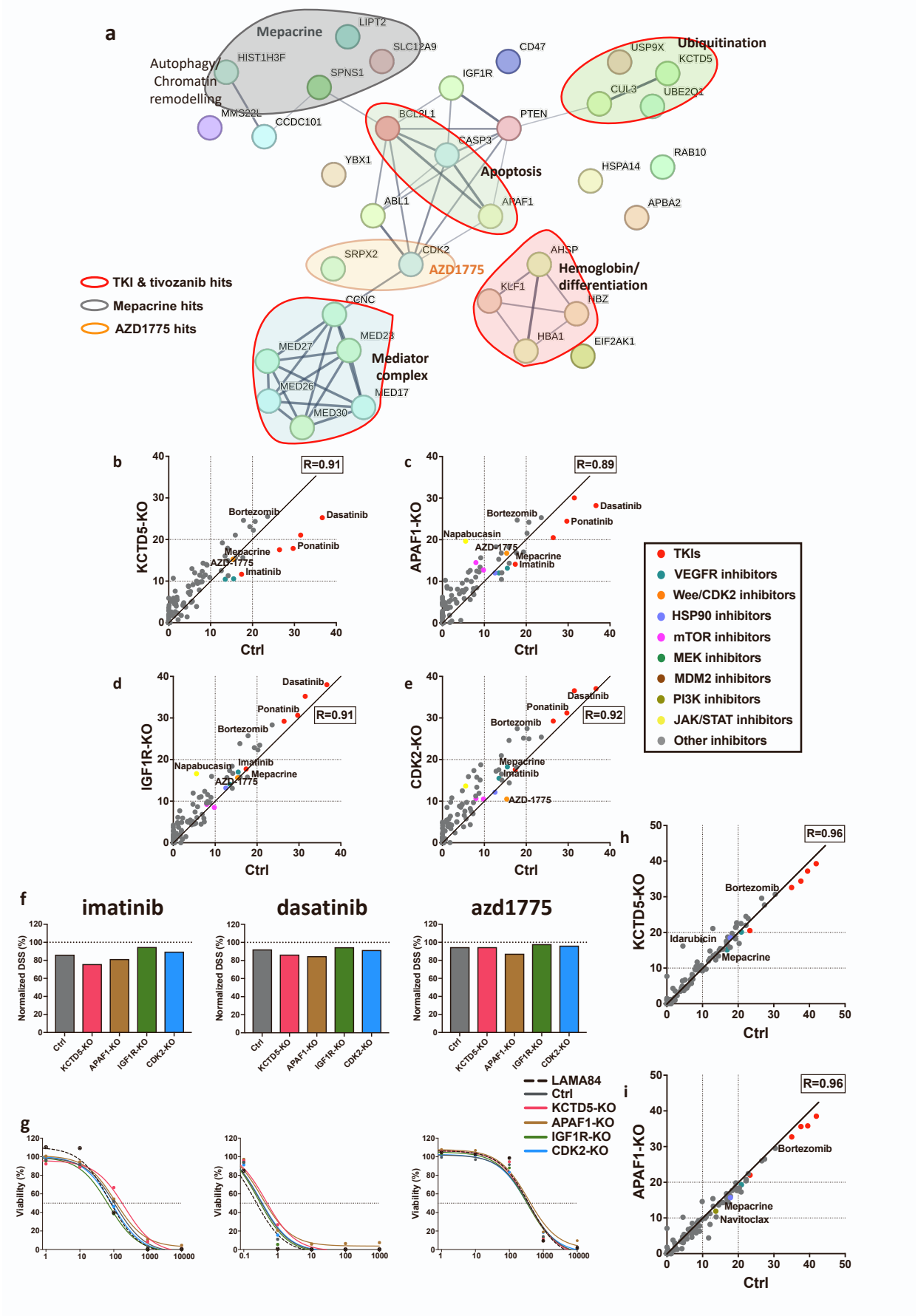

Figure S7: Genome scale CRISPR screening and individual gene CRISPR KO validation in CML cell lines. Related to Figures 4 and 5. a) Schematic figure of STRING protein interaction analysis (from the Swiss Institute of Bioinformatics [https://string-db.org/]) of resistance/sensitization hits identified by genome wide CRISPR screens and their connection with BCR-ABL. We have highlighted pathways enriched with specific drugs. b-e) Dot plot showing the correlations of DSS scores between control K562 cells (transduced with non-targeting sgRNA) and b) *KCTD5*-KO, c) *APAF1*-KO, d) *IGF1R*-KO, and e) *CDK2*-KO. All condition were tested in duplicate. Drugs are colored according to their targeting functional classes as indicated. Correlations were performed using Spearman correlation. f) Bar plots of the drug sensitivity scores of imatinib, dasatinib and azd1775 in different individual gene-KO LAMA84 cells. DSS scores were obtained from classic 72-hours DSRT experiments (see Supplemental methods) and were normalized and expressed as percentage of the drug DSS scores in parental LAMA84 cells (indicated by dashed line). CRISPR/Cas9 expressing LAMA84 cells transduced with non-targeting gRNA was used as a control (Ctrl). g) Dose-response curves of imatinib, dasatinib, and azd1775 individual gene-KO K562 cells. Dose response curve of the drugs in parental K562 cells are represented by dashed curve. Viability of the cells at different concentrations is presented as percentage of the viability of dmso treated wells. A dashed line indicates 50% viability of cells. h-i) Dot plot showing the correlations of DSS scores between control K562 cells (transduced with non-targeting sgRNA) and h) *KCTD5*-KO, and i) *APAF1*-KO. Drugs are colored according to their targeting functional classes as indicated. Data correlations were performed using Spearman correlation test.

Supplementary Figure 8

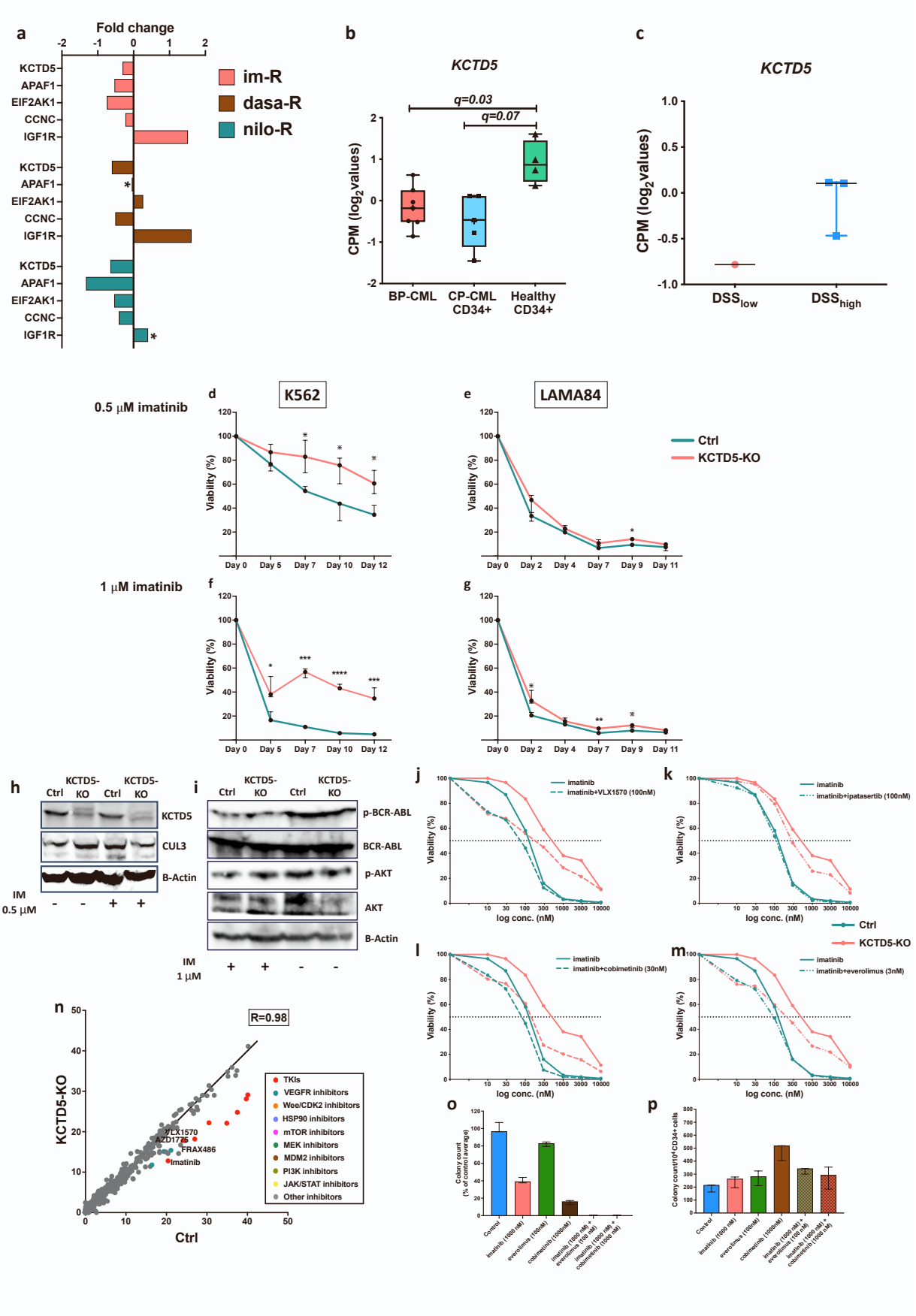

Figure S8: KCTD5-KO confers an imatinib-resistance phenotype through dysregulation of several signaling and protein processing pathways. Related to Figures 5 and 6. a) Bar plot showing fold changes in the gene expression levels of *KCTD5, APAF1, EIF2AK1, CCNC* and *IGF1R* genes in imatinib-, dasatinib- and nilotinib-resistant K562 cells from previously published gene expression data.(2) All changes in the figure were reported as significant ($q<0.05$, calculated using Cuffdiff tool) except for those marked with (*). b) Dot plot of the expression values of *KCTD5* gene in previously published transcriptional data(3) from BP, CP-LSPCs and healthy CD34+ samples (n=7, 5 and 4 respectively). Bar height represents the interquartile range, the middle line represents median values with error bars representing range. *Q-values* calculated using Bayesian statistical test. c) Dot plot of the expression values of *KCTD5* gene in previously published transcriptional data(3) from CP-LSPCs samples, that were subsetted according to imatinib DSS response into DSS-low (relatively resistant group, DSS <15, n=1) and DSS-high (sensitive group, DSS >15, n=3). The middle line represents median values with error bars representing range. d-g) Growth curves showing growth of control and KCTD5-KO K562 and LAMA84 cells in presence of different imatinib concentrations. Dots represent median values with error bars representing 95% of confidence intervals (CI). * $p<0.05$, ** $p<0.01$, *** $p<0.001$, **** $p<0.0001$, ⁎ $p<0.1$ (adjusted p value, multiple unpaired t-test corrected for multiple comparisons). h) Protein levels of KCTD5, CUL3 and B-actin proteins in untreated and imatinib-treated (0.5 μmol) control and *KCTD5*-KO K562 cell lysates. The levels of CUL3 demonstrated 1.27-fold increase and 0.44-fold decrease in imatinib-treated control and *KCTD5*-KO samples compared to untreated control samples respectively by densitometry analysis. Data is from a replicate experiment to confirm findings in Figure 6C. j) Protein levels of BCR-ABL, phosphorylated BCR-ABL (p-BCR-ABL), AKT and phosphorylated AKT (p-AKT) and B-actin proteins in untreated and imatinib-treated (1 μmol) control and *KCTD5*-KO K562 cell lysates. Densitometric analysis revealed elevation of p-AKT levels (normalized to total AKT levels) in KCTD5-KO K562 compared to control K562 cells, with ratios of 1.15 and 1.61 in presence and absence of imatinib respectively. j-k) Dose-response curves of combinations of imatinib with j) the de-ubiquitinase inhibitor VLX1570 (100 nM), k) the AKT inhibitor ipatasertib (100nM), l) the MEK inhibitor cobimetinib (30nM) and m) the mTOR inhibitor everolimus (3nM), in control (solid curves) and *KCTD5*-KO (dashed curves) K562 cells. Viability of the cells at different concentrations is presented as percentage of the viability compared to DMSO treated wells. A dashed line indicates 50% viability of cells. n) Dot plot showing the correlations of DSS scores (Pearson correlation) between control K562 cells and *KCTD5*-KO, using a 528-drug library. Drugs are colored according to their targeting functional classes as indicated. o) CFA and p) LTC-IC assay of CML-LSPCs in the presence of imatinib (1000 nM), everolimus (100 nM), and cobimetinib (1000 nM) as individual drugs and imatinib-drug combination at the indicated concentrations. Colony count output is expressed as percentage of the drug-treated conditions from control (dmso-treated) condition in CFA analysis. For LTC-IC the colony count is normalized to be expressed as colony count per 10^4 input CD34+ LSPCs.

References

1. Pietarinen PO, Eide CA, Ayuda-Durán P, Potdar S, Kuusanmäki H, Andersson EI, et al. Differentiation status of primary chronic myeloid leukemia cells affects sensitivity to BCR-ABL1 inhibitors. Oncotarget. 2017 Apr 4;8(14):22606–15. doi: 10.18632/oncotarget.15146.

2. Noel BM, Ouellette SB, Marholz L, Dickey D, Navis C, Yang TY, et al. Multiomic Profiling of Tyrosine Kinase Inhibitor-Resistant K562 Cells Suggests Metabolic Reprogramming To Promote Cell Survival. J Proteome Res. 2019 Apr 5;18(4):1842–56. doi: 10.1021/acs.jproteome.9b00028.

3. Adnan Awad S, Kankainen M, Ojala T, Koskenvesa P, Eldfors S, Ghimire B, et al. Mutation accumulation in cancer genes relates to nonoptimal outcome in chronic myeloid leukemia. Blood Adv. 2020 Feb 11;4(3):546–59. doi: 10.1182/bloodadvances.2019000943.